Electronic Characterization of the Oxidized State of the Blue Copper Protein Rusticyanin by 1 H NMR: Is the Axial Methionine the Dominant Influence for the High Redox Potential? †

ARTICLE *in* BIOCHEMISTRY · FEBRUARY 2001

Impact Factor: 3.02 · DOI: 10.1021/bi001971u · Source: PubMed

Electronic Characterization of the Oxidized State of the Blue Copper Protein Rusticyanin by ^{1}H NMR: Is the Axial Methionine the Dominant Influence for the High Redox Potential?†

Antonio Donaire,*,‡ Beatriz Jiménez,‡ José-María Moratal,§ John F. Hall,|| and S. Samar Hasnain||,⊥

Departamento de Ciencias Químicas, Universidad Cardenal Herrera-CEU, Avda, Seminario s/n, 46113-Montcada, Valencia, Spain, Departamento de Química Inorgánica, Universitat de Valencia, C/Dr. Moliner, 50, 46100-Burjassot, Valencia, Spain, The Cell Signalling Laboratory, Department of Biological Sciences, De Monfort University, The Gateway, Leicester LE1 9BH, U.K., and CCLRC Daresbury Laboratory, Warrington, Cheshire WA4 4AD, U.K.

Received August 18, 2000; Revised Manuscript Received October 30, 2000

ABSTRACT: The oxidized state of rusticyanin, the blue copper protein with the highest redox potential in its class, has been investigated through ^{1}H nuclear magnetic resonance applied to its cobalt(II) derivative. The assignment of the protons belonging to the coordinated residues has been performed. Many other amino acids situated in the vicinity of the metal ion, including six hydrophobic residues (isoleucine140 and five phenylalanines) have also been identified. The orientation of the main axes of the magnetic susceptibility tensor for the cobalt(II)-rusticyanin as well as its axial, $\Delta\chi_{ax}$, and rhombic, $\Delta\chi_{rh}$, magnetic susceptibility anisotropy components have been determined. A comparison of the present results with those previously obtained for cobalt(II)azurin [Donaire, A., Salgado, J., Moratal, J. M. (1998) *Biochemistry 37*, 8659−8673] allows us to provide further insights into the reasons for the high redox potential of this protein. According to our results, the interaction between the metal ion and the thioether Sδ of the axial methionine is not as influential as the strong destabilizing effect that the hydrophobic residues close to the metal ion undergo in the oxidized state.

Blue copper proteins (BCPs hereafter)[1] are a subclass of the copper proteins family containing analogous functional, structural, and spectroscopic features (*1*−*5*). All BCPs participate in electron transfer processes where the copper ion changes from a diamagnetic, Cu(I), to a paramagnetic, Cu(II), oxidation state. While halocyanin and auracyanin are proteins partially bound to the membrane, the rest of them are cytoplasmic or periplasmic soluble proteins. The molecular masses of all of them are in the range from 10 to 18 kDa.

The copper(II) ion in these centers presents two singular characteristics (*6*): an anomalously small parallel hyperfine coupling constant ($A_{||}$) and a very strong absorption band at ca. 600 nm, that gives these proteins their typical color. These singular features are due to a strong coordination between the copper ion and a sulfur cysteinyl atom. The metal ion coordination sphere is completed with two imidazol nitrogens from two histidines, disposed in an equatorial position, and with a sulfur thioether of a methionine in an axial position (Figure 1) (*7*). This SδMet atom is more weakly bound than the equatorial donor atoms, and it is replaced by a glutamine in stellacyanin and a leucine in laccase (*8*−*10*). In azurin, an axially and weakly bound oxygen belonging to a carbonyl group becomes a fifth ligand (*11*). The Cu−Sγ bond (Sγ of the equatorial Cys) is primarily responsible for the spectroscopic features of the copper(II) ion (*6*). In turn, the strength

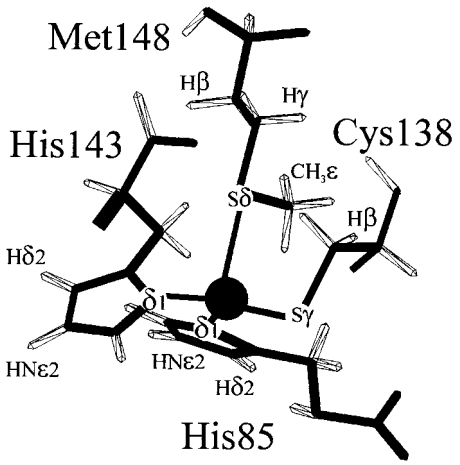

FIGURE 1: Coordination sphere of the copper ion in BCPs. In stellacyanin, the axial methionine is replaced by a glutamine. In azurin, there is another axial ligand (a carbonyl of the backbone) as a fifth ligand. The numeration of the residues refers to rusticyanin. The heavy atoms are drawn in black, while protons are displayed shadowed.

† This work has been supported with financial aid from the DGICYT-Ministerio de Educación y Ciencia, Spain (PB98-1444).

* Corresponding author: Dr. Antonio Donaire, Departamento de Ciencias Químicas, Universidad Cardenal Herrera-CEU, Avda Seminario s/n, 46113-Montcada, Valencia. Spain. Phone: 34 96 1369000; fax: 34 96 1395272; e-mail: donaire@uv.es.

‡ Universidad Cardenal Herrera-CEU.

§ Universitat de Valencia.

|| De Monfort University.

⊥ CCLRC Daresbury Laboratory.

[1] Abbreviations: NMR, nuclear magnetic resonance; BCPs, blue copper proteins; Rc, rusticyanin; CoRc, cobalt(II) rusticyanin; TOCSY, total correlation spectroscopy; NOESY, nuclear Overhauser effect spectroscopy; Az, azurin; St, stellacyanin; Am, amicyanin; PsAz, pseudoazurin; PDB, protein data bank.

10.1021/bi001971u CCC: $20.00
Published on Web 12/28/2000

of this interaction seems to be modulated by the Cu−Sδ (Sδ of the axial methionine) connection.

Concomitantly with the singular spectroscopic features of the paramagnetic copper(II) ion, the environment of copper in BCPs stabilizes the diamagnetic Cu(I) state versus the paramagnetic, Cu(II), oxidation state. Thus, the redox potentials of these proteins are higher than that one exhibited by the Cu(II)/Cu(I) pair in aqueous solution. It has been proposed that the destabilization of copper(II) arises from an atypical coordination of the copper in the active site that, in turn, must facilitate the oxidation/redox process. This is the basis for the so-called "entatic state" hypothesis proposed by Malmström at the beginning of the sixties (*12*, *13*), according to which a maximum of energy in the surroundings of the active site can be achieved due to the global folding of the protein. This idea is now widely accepted and interpreted in the sense that the copper(II) electronic structure is completely dependent on the architecture of the active center. The strained coordination of copper(II) is then considered responsible for the high redox potentials not only in BCPs but also in copper-A centers (*4*). However, the relative influence of the factors that contribute to the final destabilization of the oxidized state have not been precisely determined.

Rusticyanin (Rc, hereafter) is the BCP with the highest redox potential, 680 mV (*14*−*16*). It is present in the gram-negative bacterium *Thiobacillus ferrooxidans* (*Tf*) (*17*, *18*). This organism lives in extremely acidic media (at pH values lower than 2.5), capturing the electrons for its energy processes from the oxidation of Fe(II) to Fe(III). Rusticyanin is the most abundant protein in *Tf*, constituting the 6.5% of the total protein weight. This BCP has been proposed as the last donor of electrons to the Fe(III) in the electron-transfer chain. The three-dimensional structure of Rc has been resolved both in solid state (*19*−*21*) and in solution by NMR (*22*). The copper ion in Rc shows the characteristic coordination described above for all BCPs. A feature of Rc as revealed by the three-dimensional structure and may be highly relevant in terms of the extreme properties of this protein is the presence of several hydrophobic groups (an isoleucine and several phenylalanines) in the vicinity of the metal ion. We have recently studied the influence of the axial ligand methionine on the redox potential of Rc by site-directed mutagenesis (*23*). The substitution of this amino acid changes not only the spectroscopic properties but also the redox potential of the protein by ± 120 mV.

Nuclear magnetic resonance applied to paramagnetic molecules has been demonstrated to be a very powerful technique for obtaining structural and electronic information from the active center of BCPs (*24*−*29*). The long electronic relaxation times of the Cu(II) ion (10^{-9} s) produce very short relaxation times in protons close to it. Consequently, the broadened of the signals prevent, in most cases, their observation. Since copper(II), S = 1/2, does not show Curie relaxation, high magnetic fields (as high as 800 MHz) have recently been used to study the native oxidized protein (*27*, *28*). An alternative approach is the metal substitution of the copper(II) ion by other transition metal ions, preferably Co(II) and Ni(II) (*29*−*34*). This approach has the advantage of obtaining information not only of the ligand residues of the metal ion but also of residues close, but not coordinated, to it. The hyperfine shift (δ_{hyp}), which arises from the interaction between the nuclear and the unpaired electronic spins, contains very useful information on the electronic structure of the metal ion (*35*). This interaction produces two kinds of contributions to the hyperfine (so-called "isotropic") shift, i.e.,

$$\delta_{hyp} = \delta_{con} + \delta_{dip} \quad (1)$$

where δ_{con} (the contact or Fermi contribution) is due to the direct unpaired spin density that resides on the resonating nucleus and is transmitted through covalent bonds. δ_{dip} (the dipolar or pseudocontact contribution) is due to the dipolar interaction between the magnetic moments of the unpaired electronic spin and the resonating nucleus. This last contribution is low in systems with low magnetic anisotropy, such as copper(II) complexes. Hence, in the native oxidized protein, this information is usually lost. In contrast, for cobalt(II) derivatives of BCPs, where there are usually high levels of magnetic anisotropy (*30*, *36*), relevant information can be extracted from the dipolar contributions. This approach has been exploited in cobalt(II) azurin (*37*).

Here we present a ^{1}H NMR study of the cobalt(II) derivative of rusticyanin. Most of the hyperfine shifted signals with both contact and pseudo-contact contribution (i.e., those of the protons of the ligands of the metal ion) or with only pseudocontact contribution (i.e., those of the protons of residues close, but not bound, to the metal ion) have been assigned. The orientation and the axial, $\Delta\chi_{ax}$, and rhombic, $\Delta\chi_{rh}$, components of the magnetic susceptibility tensor anisotropy have been determined with the aim of providing a detailed molecular and electronic structure of rusticyanin and to compare the present results with those obtained for analogous systems with lower redox potentials, such as azurin, plastocyanin, pseudoazurin, or stellacyanin. We provide new information on the factors that determine the high redox potential of this protein.

MATERIALS AND METHODS

Extraction and Purification of Rusticyanin. Recombinant rusticyanin was obtained from *Escherichia coli* strains BL21-(DE3) cultures. The growth and expression of the protein was carried out as previously described (*38*). The purification procedure was followed as described elsewhere (*39*), except for the fact that no copper(II) ion was added to the samples. To measure the degree of purity in the diverse steps of the purification, copper was added to an aliquot of the extract and oxidized with potassium ferricyanide. The ratio A592/A280 was taken as a purity index, considering a value of 7.1 as optimum (the A280 value was measured before adding either copper or potassium ferricyanide to the sample). Typically, around 70−80 milligrams of protein were obtained for a culture liter.

Sample Preparation. To obtain the cobalt derivative, the solution containing the apoprotein was diluted up to ca. 5×10^{-5} M, and the pH was set at a value around 6.0−6.5. The buffer was sodium acetate 0.1 M. Cobalt(II) was added to obtain a final molar apoprotein:cobalt(II) ratio concentrations of about 1:20. Two or three days stirring at room temperature were enough to metalate more than the 90% of the apoprotein. Cobalt(II) rusticyanin (CoRc) samples were concentrated

in Millipore centricon devices. The NMR samples were typically 3−4 mM in protein (acetate buffer 0.1 M, pH 6.0).

NMR Experiments. NMR experiments were performed either in a Varian Unity400 operating at 400 MHz or in a Bruker Avance DRX500 spectrometer operating at 500 MHz. One-dimensional ^{1}H NMR experiments were performed either by using the superweft (d1-P180-d2-P90-AQ) (*40*) or the invsuperweft (d1-P180-d2-P180-d3-p90-AQ) pulse sequences. In this new pulse sequence (invsuperweft), there is one more degree of freedom than in the superweft sequence; thus, it is possible to select more adequately the three delays (Aq plus d1, d2 and d3), and then a better filter for protons with a determined T_1 can be achieved. This new pulse sequence has three substantial advantages. First, as the acquisition time can be longer than that used in the superweft sequence, a better resolution can be obtained. This point is specially relevant to observe protons that resonate in the so-called "pseudo-diamagnetic" region, i.e., between −10 and 20 ppm. Second, as the acquisition and the recycle times are longer than they are in the superweft sequence, the dispersion of the observed baseline is lower. Finally, if the three delays are properly chosen, a large number of protons within a large range of T_1 values can be filtered. This includes the water protons, which can be more effectively eliminated with this pulse sequence than with the original superweft sequence. Typical values of 4, 142, 50, and 82 ms for the d1, the d2, the d3, and the acquisition times were used. This allows us to completely eliminate protons with T_1 values higher than 100 ms.

Transversal relaxation times were obtained measuring the line broadening of the signals at half-height through the relationship $T_2^{-1} = \pi\Delta\nu_{1/2}$. Longitudinal relaxation times were obtained by using the inversion−recovery pulse sequence (d1-P180-d2-AQ) (*41*). The signal intensities were fitted to a simple exponential equation by using three parameters. 1D steady-state NOE experiments were carried out with the superweft sequence by applying, during the d2 (see above), a radio frequency on the signal of interest and interleaving the same number of scans irradiating close to, but not on, (off) the same signal, as previously described (*42*,*43*). The saturation delay was, in all cases, 40 ms. Weft-NOESY and weft-TOCSY experiments (*44*) (d1-P180-d2-NOESY and d1-P180-d2-TOCSY pulse sequence, respectively) performed in conditions to observe fast relaxing and hyperfine shifted signals were also carried out. All parameters of these experiments related with the chemical shifts, the couplings, and the acquisition times were adjusted according to the T_2 values of the observed signals, while those parameters related with dipolar couplings (mixing time in NOESY experiments) were fitted according to the T_1 of the signals, as previously described (*45*, *46*). NOESY mixing times were included in the 2−25 millisecond range.

Magnetic Susceptibility Tensor. The pseudocontact contribution to the chemical shift (eq 1) arises from the magnetic anisotropy of the system. If we assumed the metal-center point dipole approximation (*35*, *36*), it can be related with the magnetic susceptibility tensor by the expression:

$$\delta^{pc} = \frac{1}{12\pi r^3}\left[\Delta\chi_{ax}(3\cos^2\theta - 1) + \frac{3}{2}\Delta\chi_{rh}\sin^2\theta\cos 2\phi\right] \quad (2)$$

where r, θ, and ϕ are the spherical polar coordinates of a proton relative to the principal coordinates of the χ tensor. The axial, $\Delta\chi_{ax}$, and rhombic, $\Delta\chi_{rh}$, magnetic susceptibility anisotropy values are given by

$$\Delta\chi_{ax} = \chi_{zz} - \frac{1}{2}(\chi_{xx} + \chi_{yy}) \quad (3)$$

and

$$\Delta\chi_{rh} = \chi_{xx} - \chi_{yy} \quad (4)$$

In turn, χ_{xx}, χ_{yy}, and χ_{zz} are the magnitudes of the principal components of the magnetic susceptibility tensor. If we have a set of signals corresponding to protons with only pseudocontact contribution, i.e., belonging to residues close, but not coordinated, to the metal ion, it is possible to determine the orientation and the axial and rhombic magnetic susceptibility anisotropy values. The methodology followed in the determination of the orientation and magnitude of the components of the magnetic susceptibility tensor in cobalt(II) rusticyanin is completely analogous to that previously followed for cobalt(II) azurin, extensively explained in ref *37*. The program Fantasia (*47*), generously provided by Prof. Bertini (University of Florence, Italy), was applied. The diamagnetic contribution to the chemical shift was extracted from the previously reported assignment corresponding to Cu(I)Rc (*48*). This assignment was performed at pH 3.4, while in the present study the measurements have been carried out at pH 6.0. The difference in chemical shifts in Cu(I)Rc between these two conditions is minimal, as authors have checked for amide protons (lower than 0.10 ppm for all protons, data not shown). The observed hyperfine shift ranged from 2 to 3 orders of magnitude larger than this value, i.e., the committed error is completely negligible. The coordinates of rusticyanin were obtained from the pdbfiles pdba3z.ent and pdb1a8z.ent, corresponding to rusticyanin crystal structures determined by X-ray diffraction at 1.90 Å of resolution (*20*, *21*).

RESULTS AND DISCUSSION

NMR Assignments. The ^{1}H NMR spectrum of CoRc (3.5 mM, acetate buffer 0.1 M, pH 6.0) recorded with the invsuperweft pulse sequence is displayed in Figure 2. Table 1 presents a resume of the NMR parameters (hyperfine shifts, and relaxation rates) of these fast relaxing signals, as well as their assignment. These assignments were done on the basis of the dipole−dipole interaction observed in the 1D NOE and 2D NOESY experiments together with the expected distances obtained from the X-ray and solution structures (*19*−*22*). In Figure 3, panels A−H, the 1D NOE of the most hyperfine shifted signals (b, d−i, and v) are shown.

(a) Assignments of the Ligand Residues. The exchangeable downfield-shifted signals f and g have contact contribution, i.e., belong to residues coordinated to the cobalt(II) ion (Figure 1). Thus, they necessarily correspond to the NHϵ2 of the coordinated histidines. The intensity of the signal f decreases when the temperature increases, indicating that the corresponding protons exchange with the solvent at high temperatures. Hence, this proton belongs to the most exposed histidine, i.e., His143. This pattern is completely analogous to the other cobalt-substituted BCPs studied by NMR (*8*,

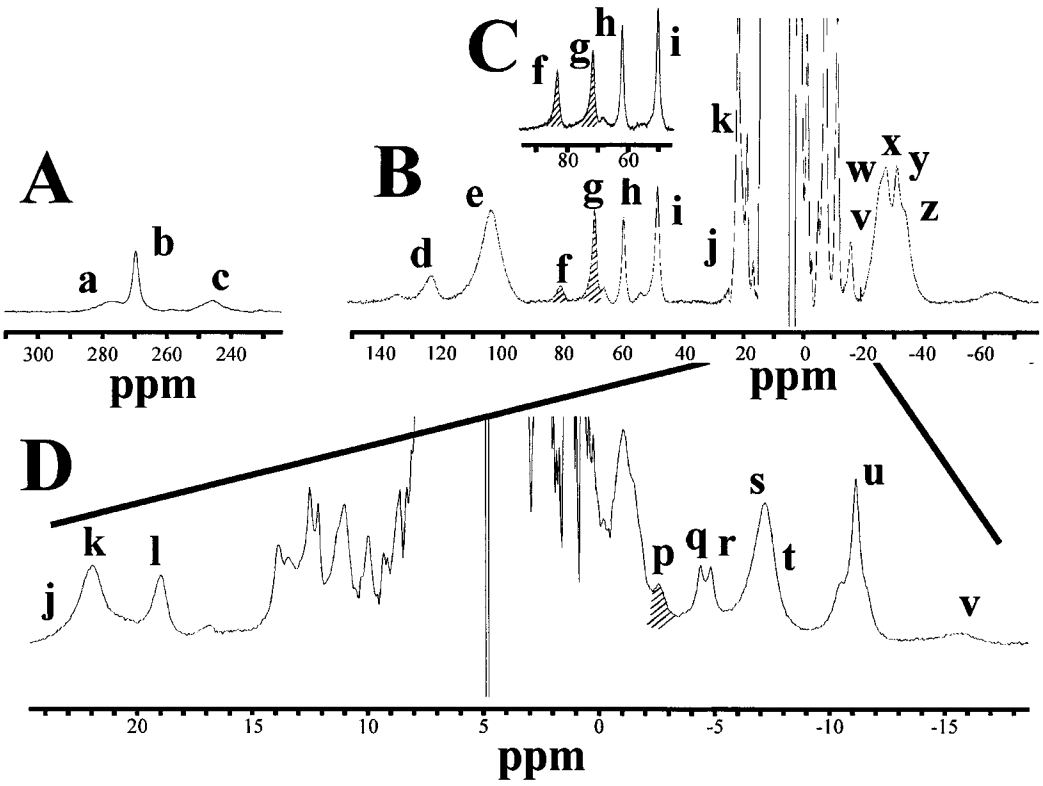

FIGURE 2: ^{1}H NMR spectrum of CoRc in acetate buffer 0.1 M, at pH 6.0 and 20 °C. (A) Far downfield (300−220 ppm) shifted region of the spectrum showing Cys138Hβ and Met148Hγ2 protons; (B) region of the spectrum displaying the rest of the signals with contact contribution; (C) CoRc ^{1}H NMR spectrum at 5 °C; (D) expansion of the so-called "pseudo-diamagnetic" (20 to −15 ppm) part of the spectrum.

25, *33*, *49*−*51*). When signal f is saturated (see Figure 3, panel D) an NOE on the signal i, among others, is observed. This permits the assignment of signal i as due to His143Hδ2. The other exchangeable signal g gives NOE with signal h (Figure 3, panel E). This allows us to assign both signals, g and h, as the Hϵ2 and Hδ2 of the coordinated His85, respectively (Figure 1). Moreover, signal v is given NOE with signal h (Figure 3, panels F and H). According to the crystal structure, this signal can be assigned to His85Hβ1. The HN peptide protons of both histidines are assigned from the strong NOEs that both HisHδ2 protons (signals h and i) are given with their respective exchangeable amide protons (see Figure 3, panels F and G).

As signal e, at 103.3 ppm, has an area that is three times that of any other peaks, it is immediately assigned to the methyl Met148CH3ϵ. Signals a, b, and c are extremely downfield shifted. This strong contact contribution is only possible for Cys138Hβ or MetHγ protons (see Figure 1). According to both crystal and solution Rc structures and to the observed T_1 and T_2 values signal b should correspond to one of the Met148Hγ protons. This is completely confirmed by the NOE experiments. In fact, this signal gives NOE with signal d (Figure 3, panel A), and thus it has to correspond to its geminal proton. Signal b also gives NOE with signals y and r (Figure 3, panel A). In turn, signal d is giving NOE with the signals r, w, and y (Figure 3, panel B). Finally, the signals r, w, and y give dipolar connectivities among them in the NOESY experiments with very short mixing times (see Supporting Information). From these experiments, it is concluded that all these signals should correspond to the same spin system, i.e., Met148. The stereospecific assignment given in Table 1 is also deduced from the same analysis. Signals a and c are consequently assigned to Cys138Hβ geminal protons.

(b) Assignments of Hydrophobic Non-Ligand Residues. In rusticyanin three-dimensional structure, an isoleucine (Ile140) and up to five aromatic residues (phenylalanines 51, 54, 76, 83, and 111) present protons within 7.5 Å from the metal ion. We have identified their corresponding resonances in the present study. For the sake of clarity in the following discussion, Figure 4, panels A−D, describe the relative disposition of these residues as well as their observed dipole−dipole connectivities. The same numeration is followed as in Figure 3, panels A−H, as well as in the NOESY experiments in Supporting Information.

Two signals of triple intensity (signals s and u, Figure 2) upfield shifted indicate the presence of two methyls very close to the metal ion. From the available three-dimensional structures, they have to belong to the residue Ile140 (Figure 4, panel A). Signals x and z give NOEs between them and very strong NOESY with the two methyl signals (see Supporting Information) suggesting they both belong to the same spin system. The NOEs between His143Hϵ2 and His143Hδ2 with IleCH$_3\delta$ (NOEs *1*, in Figure 3, panel D, and Figure 4, panel B, and *2*, in Figure 3, panel G, and Figure 4, panel B) as well as the NOESY experiments (Supporting Information) also corroborate this assignment. TOCSY experiments (see Supporting Information) are in agreement with the present assignment, although cross-peaks implicating signals s, w, and z are lost due to their line broadening. The assignment of Ile140 protons is given in Table 1.

Signal k, of triple intensity, remains folded in all the pH and temperature ranges studied, indicating that these three protons correspond to a unique spin system. This signal has

Table 1: Chemical Shifts and Relaxation Times for the Most Relevant Assigned Protons

residue	proton	signal	δ_{exp} (ppm)	T_1 (ms)	$\Delta\nu_{1/2}$ (Hz)
		Residues With Contact Contribution			
His85	HN		5.70		
	Hβ1	v	−15.78	4.3	380
	Hδ2	h	59.7	8.4	280
	Hϵ2	g	69.2	3.5	430
Cys138	Hβ	a	287	<0.4	∼3000
	Hβ'	c	260	<0.4	∼3000
His143	HN		8.95		
	Hδ2	i	48.7	7.2	330
	Hϵ2	f	80.3	1.5	620
Met148	HN		0.97		
	Hα		−1.58		
	Hβ1	y	−30.96	3.2	470
	Hβ2	w	−24.39	1.7	∼400
	Hγ1	d	122.9	1.0	1200
	Hγ2	b	285.2	1.3	800
	$CH_3\epsilon$	e	103.3	1.2	1800
Ser86	HN	p	−2.57	14.0	200
	Hα				
		Non-Ligand Hydrophobic Residues			
Phe51	Hδ		12.3		
	Hϵ,ζ	k	21.84	7.9	390
Phe54	Hδ		10.98		
	Hϵ		13.17		
	Hζ	j	22.10	6.5	
Phe76	Hδ		7.62		
	Hϵ		7.16		
	Hζ		7.40		
Phe83	Hβ1		9.07		
	Hβ2		12.1		
	Hδ	l	18.81	11.5	210
	Hϵ		12.35		
Phe111	Hδ		6.71		
	Hϵ		6.20		
Ile140	Hα		1.22		
	$CH_3\gamma$2	s	−7.25	8.7	300
	Hγ11	x	−27.38	3.2	530
	Hγ12	z	−34.35	1.7	670
	$CH_3\delta$	u	−11.24	13.0	130

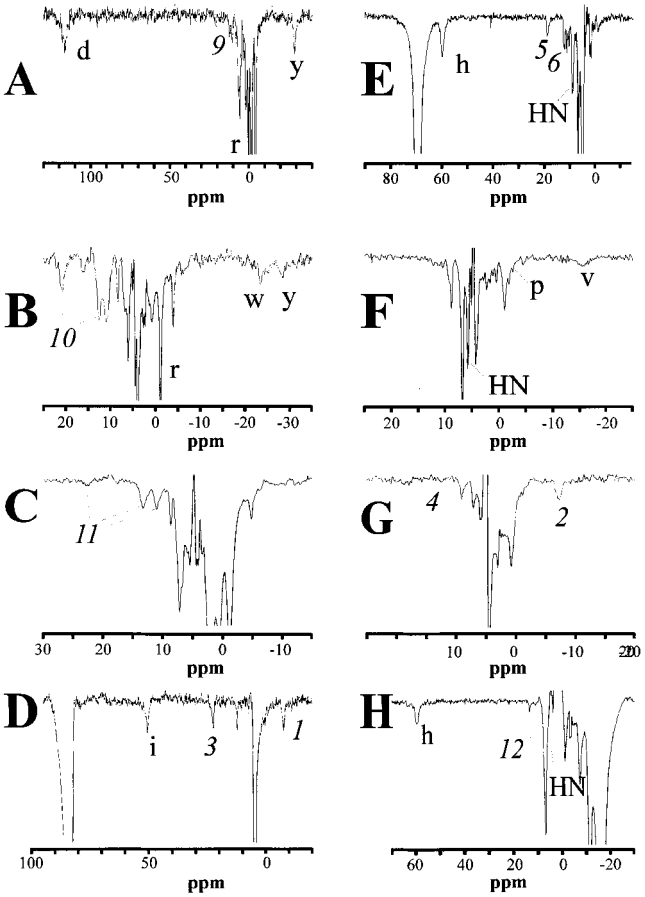

FIGURE 3: Steady-state 1D NOE difference spectra obtained after irradiating: (A) signal B, Met148Hγ2; (B) signal D, Met148Hγ1; (C) signal E, Met148$CH_3\epsilon$; (D) signal F, His143HNϵ2; (E) signal G, His85HNϵ2; (F) signal H, His85Hδ2; (G) signal I, His143δ2; (H) signal V, His85β1. Lower case letters and numbers in italics indicate the signals whose NOEs are observed. The numeration of the NOEs is the same as in Figure 4. The *x*-axis scale is different depending on the chemical shifts of the observed NOEs.

to correspond to the Hϵ and Hζ aromatic protons of a phenylalanine ring. Signal f (His143Hϵ2) gives NOE with signal k (NOE marked as *3* in Figure 3, panel D), expected between His143Hϵ2 and Phe51Hζ and Hϵ protons (Figure 4, panel B). The strong cross-peak observed in the NOESY with 7 ms of mixing time (Supporting Information) between signal k and a signal at 12.3 ppm allows us to assign Phe51Hδ protons. The NOE observed between signal i and the signal at 12.3 ppm (expected between His143Hδ2 and Phe51Hδ protons, NOE *4* in Figure 3, panel G, and Figure 4, panel B) confirms the assignment.

His85 is close enough to Phe83 to give dipolar connectivities with its aromatic ring protons. Signal g (His85Hϵ2) is giving NOE with signal l, of double intensity, and with a signal at 12.1 ppm (NOEs *5* and *6*, Figure 3, panel E, and Figure 4, panel C). The analysis of the NOESY and TOCSY experiments (Supporting Information) indicates that these signals have to arise from Phe83Hδ and Hβ2 protons. Several dipolar connectivities observed between the aromatic rings of Phe51 and Phe83 (NOEs 7 and 8, Figure 4, panel C) are observed in the corresponding NOESY, confirming the assignment.

In a similar way, Phe54, close to the ligand Met148, is assigned. In Figure 4, panel D, the dipole−dipole connectivities expected between these two amino acids are marked with the numbers *9*−*11*. The corresponding experimental NOEs are marked with the same numbers in Figure 3, panel A−C. The NOEs of Met148Hγ1 and $CH_3\epsilon$ with Phe54Hζ allow us to identify signal j, a fast relaxing proton under signal k (the existence of this signal is clearly identified at 10 °C, data not shown). The line broadening of cross-peaks implicating Phe54 clearly indicates that the aromatic ring of this phenylalanine is in slow exchange on the NMR time scale at 20 °C. Phe76 is identified from the NOEs observed with His85β1 (NOE *12* in Figure 3, panel H, and Figure 4, panel C). Finally, Phe111 assignment is obtained from the NOESY between Ile140CH3δ2 and a signal at 6.71 ppm (data not shown). For these two amino acids (Phe76 and Phe111), TOCSY experiments were successful in corroborating the assignment.

(c) Other Assignments. The exchangeable upfield-shifted signal p is assigned to Ser86HN due to the NOE connectivities observed with both His85 Hδ2 and Hβ1 protons (see Figure 3, panels F and H, respectively). Ala44, Val45, Pro52, Ser53, Asn80, Gly84, and Gly142 were assigned from the NOESY connectivities with the previously assigned residues in conjunction to the NOESY and TOCSY connectivities. In Supporting Information, cross-peaks and spin patterns implicating these residues are indicated with the same

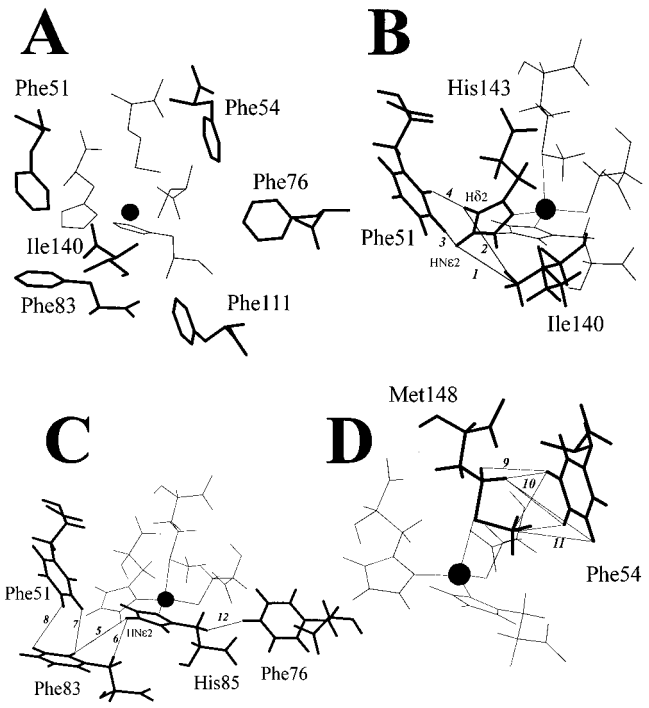

FIGURE 4: (A) Overview distribution of the apolar residues close to the metal ion (Ile140, and phenylalanines 51, 54, 76, 83, and 111, in black). The rest of the figures (in which the protons are included) represent the expected NOEs implicating some protons of these apolar residues and (B) His143, (C) His85, and (D) Met148. Rc coordinates have been taken from the a3zpdb.ent file. The numeration of the NOEs is the same as in Figure 4. In all the figures, the four ligands are displayed (with thick lines) for a better comprehension of the relative orientation of the residues.

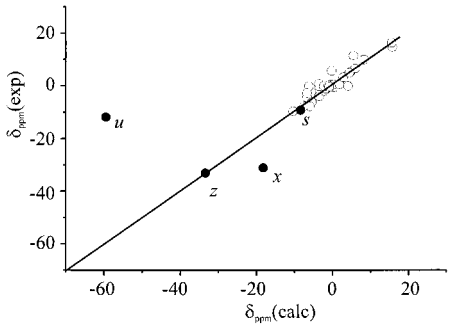

FIGURE 5: Plot of the experimental versus calculated dipolar shifts in CoRc. The points marked in dark correspond to Ile148 protons (signals u, s, x, z). They have not been included in the calculations (see text).

numbers as the position of the residue in the amino acid sequence of the protein.

Determination of the Magnetic Susceptibility Tensor. The assignment of 34 protons belonging to noncoordinated residues allows us to calculate the orientation of the main axes of the magnetic susceptibility tensor of CoRc as well as the magnitude of its magnetic susceptibility anisotropy components. In Figure 5, the calculated versus the experimental dipolar shifts for these 34 protons are shown. These values together with the assignment of each signal are reported in Supporting Information. If we eliminate Ile140 protons from the analysis, a good agreement between the calculated and the experimental δ_{dip} data is observed, with a good value for the linear regression coefficient (0.93). These data clearly indicate the applicability of the metal-centered model (eq 2) to our system.

As it was just commented, some protons of Ile140 do not fit well with the values calculated by applying eq 2 and by using any of the available (crystal or solution) three-dimensional structures of Rc. In fact, while there is an acceptable fit for IleHN, Hα, Hγ12, and CH3γ2 protons, Ile140 CH3δ methyl and Ile140Hγ11 proton are clearly in disagreement with the calculated data (see Figure 5). According to its expected value, the signal corresponding to Ile140$CH_3\delta$ (signal *u*) should appear much more upfield shifted (at -51 ppm) than it appears (-11.2 ppm). In contrast, Ile140Hγ11 (signal x) should appear much more downfield shifted (at -17 ppm) than it appears (-31 ppm). The T_1 values of these two protons are also different from those values expected from their distances to the metal ion. In fact, if we compare the longitudinal relaxation times of protons whose signals are resolved, the Ile140Hγ11 proton should show a higher T_1 value (higher than 5 ms, instead of the observed 3.2 ms value, Table 1). In contrast, Ile140$CH_3\delta$, at 4.1 Å from the metal ion, should have a much shorter T_1 value (lower than 5 ms, instead of the experimental value of 13.0 ms, Table 1). This takes us to the conclusion that Ile140 side chain is, at least in our working conditions, in a different relative position with regard to the metal ion as compared to that found in the previously obtained three-dimensional structures of Rc. In these structures, the dihedral angle Cα-Cβ-Cγ-Cδ of Ile140 has a value of (177 $\pm$ 8)°. We have calculated the pseudocontact contribution for Ile $CH_3\delta$ methyl protons changing this dihedral angle between 177° and $\pm$ 180° in steps of 10° and leaving the rest of the structure unchanged. If we assumed a value of -130° (i.e., a rotation of $+53$°) for this angle, the expected value of its dipolar shift would be -14.5 ppm and the distance to the metal ion would be 5.3 Å. These two values would be in good agreement with our experimental results. On the other hand, if we carefully examine the orientation of the Ile140 side chain in the available family of the solution structures (1cur.ent pdbfile) we realize that two of them (structures 17 and 23) have the same orientation and proton−metal ion distances as we expect from our present study. This means that the present data are consistent with the experimental restraints used in the solution structure determination (*22*). Therefore, it is probable that a conformational change implicating this dihedral angle takes place in solution. Since paramagnetic NMR is much more sensible to local conformation changes for residues close to the metal ion than diamagnetic NMR, we then conclude that this is the main (if not the only one) Ile140 side chain orientation in our working conditions. This conformational change of Ile140 could be relevant in the hydrophobicity environment of the metal ion (see below).

In Table 2, the angles that the main axes of the magnetic susceptibility tensor form with the bonds between the metal ion and the coordinated atoms are given. The calculated magnetic susceptibility anisotropy components are also given. In Figure 6, the orientation of these axes with respect to the four bonds of the cobalt ion is displayed. In both cases, the analogous data for cobalt(II) azurin are also reproduced (from ref *37*). The first evident result is the large degree of concordance between the orientation of the magnetic axes in both cobalt(II) metalo-derivatives (see Table 2). We can clearly conclude that the orientation of the magnetic susceptibility tensor in CoRc is analogous in CoAz, and thus,

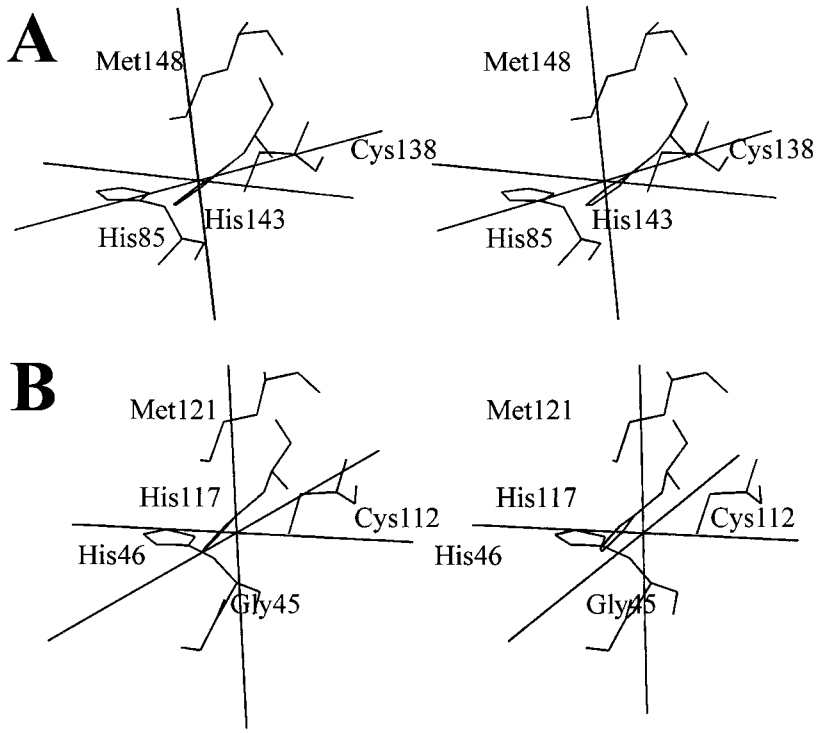

FIGURE 6: Stereoview representation of the principal axes of the magnetic susceptibility tensor with respect to the metal−ligand bonds for (A) CoRc and (B) CoAz (from ref 37).

Table 2: Angles (in Degrees) of the Main Axes of the Magnetic Susceptibility Tensor with Respect to the Bonds between the Metal Ion and the Coordinated Atoms for Cobalt(II) Rusticyanin[a] and for Cobalt(II) Azurin[b]

	CoRc			
	Met148Sδ	Cys138Sγ	His85Nδ1	His143Nδ1
χ_{xx}	73 ± 4	100 ± 4	37 ± 4	139 ± 4
χ_{yy}	99 ± 4	155 ± 4	55 ± 4	49 ± 4
χ_{zz}	160 ± 5	68 ± 5	80 ± 5	94 ± 5
$\Delta\chi_{ax}$ ($m^3 \times 10^{32}$)	-5.3 ± 0.3			
$\Delta\chi_{rh}$ ($m^3 \times 10^{32}$)	-5.1 ± 0.3			
	CoAz			
	Met121Sδ	Cys112Sγ	His46Nδ1	His117Nδ1
χ_{xx}	92 ± 4	96 ± 4	37 ± 4	139 ± 4
χ_{yy}	83 ± 5	174 ± 5	54 ± 5	51 ± 5
χ_{zz}	159 ± 4	91 ± 4	95 ± 4	81 ± 4
$\Delta\chi_{ax}$ ($m^3 \times 10^{32}$)	-6.8 ± 0.3			
$\Delta\chi_{rh}$ ($m^3 \times 10^{32}$)	2.8 ± 0.1			

[a] Calculated magnetic susceptibility anisotropy components are given as well. [b] Values for CoAz are obtained from ref *37*.

the orientation of the molecular orbitals in both cobalt metalo-substituted BCPs also is essentially the same. As it was indicated in the introduction section (Figure 1), the interaction Co−SδMet is much stronger in CoRc than in CoAz. Our present results indicate that this different strength of the axial interaction does not alter the overall electronic structure of the metal ion.

The values of $\Delta\chi_{ax}$ and $\Delta\chi_{rh}$ are both quite large, expected when zero-field splitting (ZFS) effects are present. In highly symmetrical tetrahedral Co(II) complexes, the ground state is a term A_2, orbitally nondegenerate. In these cases, the expected magnetic anisotropy is very low, and, consequently, a very low dispersion would be observed in the pseudo-diamagnetic region of the ^{1}H NMR spectrum. This is not our case. Hence, even if cobalt(II) is four-coordinated in Rc (as is clearly the case), low symmetry components are present, giving a large degree of magnetic anisotropy. This suggest a C_s symmetry for the cobalt(II) more than a tetrahedral one as occurs in the native oxidized protein, and it corroborates the fact that cobalt(II) in Rc has a very similar coordination sphere to copper(II) in Rc.

Residues with Contact Contribution. The pseudocontact and contact contributions of protons belonging to the coordinated residues are displayed in Table 3. Again we have also included the corresponding data for CoAz from ref *37*. Data for Ser86 (Asn47 in azurin) protons, having contact contribution, are also reported.

In contrast with the chemical shift values of Gly46 in azurin, the contact contribution of Gly84 is negligible, indicating that the carbonyl group of this amino acid is not coordinated in cobalt rusticyanin. This confirms that cobalt-(II) in Rc has the same coordination as the copper(II) ion in the native Rc (see Figure 1). This coordination (in both native or cobalt derivatives) is different to that present in azurin. On the other hand, the chemical shifts implicating the axial methionine protons (Met148 in Rc, Met120 in Az) display large and very evident differences in both derivatives. Met148$CH_3\epsilon$ methyl protons show a contact contribution of 106 ppm larger in CoRc than in CoAz. Moreover, the contact contributions of Met$H\gamma$1 and $H\gamma$2 protons are higher in CoRc than in CoAz by values of 68 and 300 ppm, respectively. This conclusive data reflects the much stronger bond of the metal ion to the axial methionine in Rc than in Az. In fact, in the native Rc the Cu−SδMet distance is 2.75 Å, while in azurin this distance is 3.2 Å. The contact contribution of these axial methionine protons depends on the unpaired spin density on the resonating nuclei (that, in turn, reflects the strength of the covalent bond) and on the dihedral angle of the implicated covalent bonds (*52*, *53*). For the Met148$CH_3\epsilon$

Table 3: Calculated Dipolar and Contact Contributions for the Hyperfine Shifts of the Protons of the Coordinated Residues for the Cobalt(II) Derivatives of Rusticyanin and Azurin[a]

		CoRc		CoAz	
residue	proton	δ_{dip} (ppm)	δ_{con} (ppm)	δ_{dip} (ppm)	δ_{con} (ppm)
Gly84(85)[b]	HN			−9.80	10.7
	Hα1			−10.53	54.2
	Hα2			−26.71	−5.9
His85(46)	HN	−11.8	11.47	−11.22	−6.1
	Hβ1	−8.5	−11.22	7.08	5.6
	Hδ2	−1.9	53.6	7.75	37.3
	Hε2	10.3	44.2	16.56	46.9
Cys138(112)	Hβ	69.9	205	5.38	223.2
	Hβ′	59.7	184	−5.27	287.4
His143(117)	HN	−3.79	1.1	2.56	3.2
	Hδ2	3.4	38.5	7.18	42.3
	Hε2	19.9	48.9	7.47	46.8
Met148(121)	HN	−6.3	−1.6	−5.52	−1.8
	Hα	−7.37	1.75	−9.93	2.5
	Hβ1	−23.2	−9.8	−25.93	5.3
	Hβ2	−13.5	−17.4	−26.85	6.1
	Hγ1	−11.5	132.5	−19.53	64.4
	Hγ2	−19.2	301.6	−20.22	−0.3
	CH_3ε	−16.9	130.3	−31.21	24.0
Ser86(Asn47)	HN	15.9	−26.5	30.1	−33.6
	Hα	4.7	3.2	5.36	5.3

[a] Ser86 backbone protons, which have contact contribution, are included in the table. [b] Numbers between parentheses indicate the residue in azurin.

methyl protons, there is no dependence on the dihedral angle. Thus, we can estimate an average value for the covalent contribution of 65 ppm for CoRc while in CoAz the analogous contribution only represents 12 ppm. This means that there is roughly 5 times more covalence in the Co−Sδ(axial methionine) bond in CoRc than in CoAz.

Met148Hγ protons experience the unpaired spin density in the same magnitude as MetCH_3ε methyl protons, although, in this case, a dihedral angle dependence shown has to be operative. Taking the average $\delta_{av} = (\delta_{conH\gamma1} + \delta_{conH\gamma2})/2$ (*34*) for the contact contributions of the two methylene Hγ protons, a value of 216 ppm for the covalent contribution to the hyperfine shift is obtained (Table 3). Again, we have to compare this value with that obtained for CoAz Met121Hγ protons (32 ppm, Table 3). Thus, the degree of covalence of the Co−Sδ(axial methionine) bond is around 6 times higher for CoRc than for CoAz, consistent with the data obtained for the methyl protons (see above).

Two other points can be emphasized from Table 3. First, contact contribution for Cys138Hβ protons is lower in CoRc than it is in CoAz. This is consistent with a lower interaction in the first derivative. The average $\delta_{av} = (\delta_{conH\beta} + \delta_{conH\beta'})/2$ for the contact contributions of the two CysHβ protons in both CoRc and in CoAz (195 and 255 ppm, respectively) gives a 20% higher degree of covalence for CoAz than for CoRc. Second, Ser86 HN (Asn47 in CoAz), forming hydrogen bond with Cys138Sδ atom, has roughly the same (negative) contact contribution in both metallo-derivatives. Hence, even when the charge of these two amino acids is different, the contribution to the electronic structure of the metal seems to be similar. Finally, imidazol rings of the two coordinated histidines in both proteins (CoRc and CoAz) seem to have similar unpaired spin density.

Comparison with Other Cobalt Substituted BCPs. Recently, the ^{1}H NMR spectra of Co(II) amicyanin. CoAm (*51*), and Co(II) pseudoazurin, CoPs (A. Vila, personal communication) have been reported and assigned. In the case of CoPs, the axial methionine protons have very similar chemical shifts to those ones shown by CoRc in the present paper (the difference in the chemical shifts for the analogous protons of coordinated residues are lower than a 10% of their chemical shifts values). This is due to a similar orientation as well as to a similar strength of the metal−methionine interaction (*19*, *54*). On the contrary, CoAm (as CoAz), with a clear different disposition of the axial methionine in the structure, shows completely different chemical shifts for the axial methionine protons as compared to the CoRc or the CoPs methionine chemical shifts. This indicates that the way in which the metal and methionine interact is decisive in the unpaired spin density residing on the methionine. However, the orientation of the magnetic susceptibility tensor (see above) and, hence, the electronic structure of the cobalt(II) ion, is essentially the same in both CoRc and CoAz, even when the interaction between the metal ion and the methionine is completely different in the proteins. Moreover, in all CoBCPs substituted proteins whose NMR spectra have been recorded (*37* and refs therein), the distribution of the assigned protons clearly indicates a similar orientation of the magnetic susceptibility tensor. This strongly suggests a similar electronic structure for all of them, independently of the axial methionine interaction and its orientation.

Implications in the High Redox Potential of Rusticyanin. The degree of covalence between the metal ion and the axial methionine is thought to be one of the main determinants for modulating the interaction between the metal ion and the CysSγ atom (*4*, *6*, *23*, *55*). In fact, as previously commented, the substitution of the axial methionine in Rc by other amino acids of different polarity modifies the redox potential of the protein (*23*). However, the total span of the redox potentials in these mutants at a fixed pH value (pH 6.2) is 250 mV (from 363 mV for the RcE148 mutant to 613 mV for the RcL148 mutant, *23*), while the span of the redox potentials in BCPs is 500 mV (from 185 mV for stellacyanin to 680 mV for Rc). Our present data clearly demonstrate that the methionine axial interaction is clearly different in CoRc to CoAz. However, in both cases this different interaction seems not to alter the electronic distribution and orientation of the orbitals with unpaired spin density of the cobalt ion. On the other hand, rusticyanin and pseudoazurin (whose cobalt derivatives have almost superimposable ^{1}H NMR spectra) redox potentials differ by a value as large as 400 mV. Then, it is clearly concluded that the different degree of the strength in the metal ion−axial methionine interaction is not the primary cause of the high redox potential found in rusticyanin.

On the contrary as observed in Figure 5, panel A, several hydrophobic residues are in the immediate vicinity of the metal ion. Particularly, Ile140 is an apolar residue sited very close to the metal ion that prevents the access of the water to the metal ion. This residue is not present in other BCPs, and its interaction with the metal ion has been proposed to be a crucial factor responsible for the high redox potential of this protein (*19*, *22*, *23*). From our present data, it is clearly observed that the effect of unpaired electrons on these residues is evident since all of them experience large dipolar contributions in their chemical shifts. Analogously, these hydrophobic residues have strong dipole−dipole interactions

with the unpaired spin electron(s). As it has been previously reported (not only for rusticyanin in the case of BCPs but also for other systems containing metal ions, such as ferredoxins and high potential iron proteins, *56*), the hydrophobicity of the metal ion and its accessibility to the solvent are the determinant factors in the redox potential of metalloproteins. The dipole−dipole interactions between the resonating nuclei and the metal ions (observed in the present study by paramagnetic NMR) heavily influences the relative stability of different oxidation states of the copper, with the higher resident charge on the cupric ion, causing greater destabilization. Our present work clearly corroborates previous studies (*19*, *22*, *23*) in the sense that this dipolar effect is the most significant factor in determining the high redox potential of this protein.

CONCLUSIONS

We have characterized the electronic structure of the metal ion in the cobalt(II)-substituted rusticyanin by ^{1}H NMR. We have determined the magnetic susceptibility anisotropy components and the orientation of its main axes. These have allowed us to obtain the degree of the contact contribution to the chemical shifts of the protons belonging to the ligand residues, specially those of the axial ligand Met148. This, in turn, has allowed us to estimate the degree of covalence for the Co−Sδ(Met148) interaction. This interaction is found to be stronger in CoRc than in CoAz in agreement with the crystallographic structures. However, the electronic structure of the metal ion is roughly the same in both metal-substituted BCPs. The presence of the hydrophobic residues has been suggested as a possible reason for the very high redox potential. The effect of unpaired electrons on these hydrophobic residues is evident in the form of large dipolar contributions in their chemical shifts. We suggest that this dipolar effect is a significant factor in determining the high redox potential of this protein.

ACKNOWLEDGMENT

We thank Drs. Alejandro J. Vila (University of Rosario, Argentina) and Claudio Fernández (University of Buenos Aires, Argentina) for proportioning us their results on cobalt(II) pseudoazurin, as well as for many helpful discussions.

SUPPORTING INFORMATION AVAILABLE

Three figures displaying two weft-NOESY experiments (with 7 and 15 ms of mixing times, respectively) and a TOCSY experiment (with 35 ms of mixing time) are given. A table with the experimental and expected (according to eq 2) chemical shifts of the assigned protons are also included. This material is available free of charge via the Internet at http://pubs.acs.org.

REFERENCES

1. Adman, E. T. (1991) *Adv. Prot. Chem. 42*, 145−197.
2. Sykes, A. G. (1991) in *Advances in Inorganic Chemistry* (Sykes, A. G., Ed.) pp 377−408, Academic Press, New York.
3. Messerschimdt, A. (1998) *Struct. Bonding 90*, 37−68.
4. Randall, D. W., Gamelin, D. R., LaCroix, L. B., and Solomon, E. I. (2000) *J. Biol. Inorg. Chem. 5*, 16−29.
5. Gray, H. B., and Winkler, J. R. (1996) *Annu. Rev. Biochem. 65*, 537−561.
6. Solomon, E. I., Baldwin, M. J., and Lowery, M. D. (1992) *Chem. Rev. 92*, 521−542.
7. Nar, H., Messerschimdt, A., Huber, R., van de Kamp, M., and Canters, G. W. (1991) *J. Mol. Biol. 221*, 765−772.
8. Vila, A. J., and Fernandez, C. O. (1996) *J. Am. Chem. Soc. 118*, 7291−7298.
9. Hart, P. J., Nersissian, A. M., Herrmann, R. G., Nalbandyan, R. M., Valentine, J. S., Eisenberg, D., (1996) *Protein Sci. 5*, 2175−2183.
10. Ducros, V., Brzozowski, A. M., Wilson, K. S., Brown, S. H., Ostergaard, P., Schnieder, P., Yaver, D. S., Pederson, A. H., and Davies, G. J. (1998) *Nat. Struct. Biol. 5*, 310−316.
11. Baker, E. N. (1988) *J. Mol. Biol. 203*, 1071−1095.
12. Malmström, B. G. (1965) in *Oxidases and Related Redox Systems* (King, T. E., Mason, H. S., and Morrison, M., Eds.) pp 207−216, Wiley, New York.
13. Malmström, B. G. (1994) *Eur. J. Biochem. 233*, 711−718.
14. Ingledew, W. J., and Cocco, D. (1980) *Biochim. Biophys. Acta 590*, 141−158.
15. Lappin, A. G., Lewis, C. A., and Ingledew, W. J. (1985) *Inorg. Chem. 24*, 1446−1450.
16. Blake, R. C., White, K. J., and Shute, E. A. (1991) *Biochemistry 30*, 9443−9449.
17. Ingledew, W. J., Cox, J. C., and Halling, P. J. (1977) *FEMS Microbiol. Lett. 2*, 193−197.
18. Ronk, M., Shively, J. E., Shute, E. A., and Blake, R. C. (1991) *Biochemistry 30*, 9435−9442.
19. Walter, R. L., Ealick, S. E., Friedman, A. M., Blake, R. C., Proctor, P., and Shoham, M. (1996) *J. Mol. Biol. 263*, 730−751.
20. Shoham, M. (1992) *J. Mol. Biol. 227*, 581−582.
21. Harvey, I., Hao, Q., Ingledew, W. J., and Hasnain, S. S. (1998) *Acta Crystallogr. D 54*, 629−635.
22. Botuyan, M. A., Toy-Palmer, A., Chung, J., Blake, R. C., Beroza, P., Case, D. A., and Dyson, H. J. (1996) *J. Mol. Biol. 263*, 752−767.
23. Hall, J. F., Kanbi, L. D., Strange, R. W., and Hasnain, S. S. (1999) *Biochemistry 38*, 12675−12680.
24. Moratal, J. M., Salgado, J., Donaire, A., Jimenez, H. R., and Castells, J. (1993) *J. Chem. Soc., Chem. Commun.* 110−112.
25. Salgado, J., Jimenez, H. R., Donaire, A., and Moratal, J. M. (1995) *Eur. J. Biochem. 231*, 358−369.
26. Vila, A. J. (1994) *FEBS Lett. 355*, 15−18.
27. Bertini, I., Ciurli, S., Dikiy, A., Luchinat, C., Martini, G., and Safarov, N. (1999) *J. Am. Chem. Soc. 121*, 2037−2046.
28. Bertini, I., Fernandez, C. O., Karlson, B. G., Leckner, J., Luchinat, C., Malmström, B. G., Nersissian, A. M., Pierattelli, R., Shipp, E., Valentine, J. S., and Vila, A. J. (2000) *J. Am. Chem. Soc. 122*, 3701−3707.
29. Salgado, J., Kalverda, A. P., Dennison, C., and Canters, G. W. (1996) *Biochemistry 35*, 3085−3092.
30. Donaire, A., Salgado, J., Jimenez, H. R., and Moratal, J. M. (1995) in *Nuclear Magnetic Resonance of Paramagnetic Macromolecules* (La Mar, G. N., Ed.) pp 213−244, Kluwer Academic Publishers, Dordretch.
31. Fernandez, C. O., Sannazzaro, A. I., and Vila, A. J. (1997) *Biochemistry 36*, 10566−10570.
32. Fernandez, C. O., Sannazzaro, A. I., Diaz, L. E., and Vila, A. J. (1998) *Inorg. Chim. Acta 273*, 367−372.
33. Salgado, J., Jimenez, H. R., Moratal, J. M., Kroes, S. J., Warmerdam, G. C. M., and Canters, G. W. (1996) *Biochemistry 35*, 1810−1819.
34. Vila, A. J., Ramirez, B. E., Di Bilio, A. J., Mizoguchi, T. J., Richards, J. H., and Gray, H. B. (1997) *Inorg. Chem. 36*, 4567−4570.
35. Bertini, I., and Luchinat, C. (1996) in *NMR of Paramagnetic Substances*, Coord. Chem. Rev. 150, Elsevier, Amsterdam.
36. Bertini, I. and Luchinat, C. (1986) in *NMR of Paramagnetic Molecules in Biological Systems*, Benjamin/Cummings, Menlo Park, CA.
37. Donaire, A., Salgado, J., and Moratal, J. M. (1998) *Biochemistry 37*, 8659−8673.
38. Hall, J. F., Hasnain, S. S., and Ingledew, W. J. (1996) *FEMS Microbiol. Lett. 137*, 85−89.

39. Hall, J. F., Kanbi, L. D., Harvey, I., Murphy, L. M. M., and Hasnain, S. S. (1998) *Biochemistry 37*, 11451−11458.
40. Inubushi, T., and Becker, E. D. (1983) *J. Magn. Reson. 51*, 128−133.
41. Vold, R. L., Waugh, J. S., Klein, M. P., and Phelps, D. E. (1968) *J. Chem. Phys. 48*, 3831−3832.
42. Emerson, S. D., Lecomte, J. T. J., and La Mar, G. N. (1988) *J. Am. Chem. Soc. 110*, 4176−4182.
43. Banci, L., Bertini, I., Luchinat, C., Piccioli, M., Scozzafava, A., and Turano, P. (1989) *Inorg. Chem. 28*, 4650−4656.
44. Chen, Z. G., de Ropp, J. S., Hernandez, G., and La Mar, G. N. (1994) *J. Am. Chem. Soc. 116*, 8772−8783.
45. Banci, L., Bertini, I., Luchinat, C., Messori, L., and Turano, P. (1993) *Appl. Magn. Reson. 4*, 461−476.
46. Banci, L., Bertini, I., and Luchinat, C. (1994) in *Methods Enzymol.* (James, T. L. and Oppenheimer, N. J., Eds.) Vol. 239, pp 485−514, Academic Press, Inc., London.
47. Banci, L., Bertini, I., Bren, K. L., Cremonini, M. A., Gray, H. B., Luchinat, C., and Turano, P. (1996) *JBIC, J. Biol. Inorg. Chem. 1*, 117−126.
48. Hunt, A. H., Toy-Palmer, A., Cavanagh, J., Blake, R. C., II, and Dyson, H. J. (1994) *J. Mol. Biol 244*, 370−384.
49. Moratal, J. M., Salgado, J., Donaire, A., Jimenez, H. R., and Castells, J. (1993) *Inorg. Chem. 32*, 3587−3588.
50. Piccioli, M., Luchinat, C., Mizoguchi, T. J., Ramirez, B. E., Gray, H. B., and Richards, J. H. (1995) *Inorg. Chem. 34*, 737−742.
51. Salgado, J., Kalverda, A. P., Diederix, R. E. M., Canters, G. W., Moratal, J. M., Lawler, A. T., and Dennison, C. (1999) *JBIC, J. Biol. Inorg. Chem. 4*, 457−467.
52. Karplus, M. (1963) *J. Am. Chem. Soc. 85*, 2870−2871.
53. Bertini, I., Capozzi, F., Luchinat, C., Piccioli, M., and Vila, A. J. (1994) *J. Am. Chem. Soc. 116*, 651−660.
54. Cunane, L. M., Chen, Z. W., Durley, R. C. E., and Mathews, F. S. (1996) *Acta Crystallogr. D 52*, 676−686.
55. Wittung-Stafshede, P., Hill, M. G., Gomez, E., Di Bilio, E., Karlsson, B. G., Leckner, J., Winkler, J., Gray, H. B., and Malmstrom, B. G. (1998) *JBIC, J. Biol. Inorg. Chem. 3*, 367−370.
56. Beinert, H. (2000) *JBIC, J. Biol. Inorg. Chem. 5*, 2−15 (and references therein).

BI001971U